Journal of Cerebral Blood Flow & Metabolism (2012) 32, 2012–2022

www.jcbfm.com

JCBFM Open

Albumin therapy enhances collateral perfusion after laser-induced middle cerebral artery branch occlusion: a laser speckle contrast flow study

Richard A DeFazio[1,4], Weizhao Zhao[2], Xiaolu Deng[1], Andre Obenaus[3] and Myron D Ginsberg[1]

[1]*Department of Neurology, University of Miami Miller School of Medicine, Miami, Florida, USA;*
[2]*Department of Biomedical Engineering, University of Miami, Coral Gables, Florida, USA;*
[3]*Department of Pediatrics, Loma Linda University, Loma Linda, California, USA*

Laser speckle contrast (LSC) was used to compare the extent of cortical ischemia in two inbred mouse strains that differed in their degree of collateral circulation, after laser occlusion of the distal middle cerebral artery, and after treatment with 25% albumin (ALB) or saline (control). Sequential LSC images acquired over ~90 minutes were coaligned, converted to relative flow, and normalized to baseline. After 3-day survival, infarction was quantified by triphenyl tetrazolium chloride or magnetic resonance imaging. In the sparsely collateralized BALB/c strain, mean flow fell to 13% to 14% and 33% to 34% of baseline in central (core) and peripheral (penumbral) regions of interest, and ALB treatment at 30 minutes enhanced perfusion in both regions by ~2-fold relative to saline, restoring flow to the benign-oligemic range centrally, and to the hyperemic range peripherally. The ALB-induced increment in parenchymal perfusion was disproportionate to the subtle flow increase in the occluded artery itself, suggesting that ALB improved collateral circulation. Cortical infarction in BALB/c mice was reduced 45% by ALB treatment. In contrast to BALB/c mice, the better-collateralized CD-1 strain developed milder ischemia, had smaller infarcts, and showed no differential benefit of ALB. We conclude that where native collateralization is insufficient (BALB/c strain), ALB treatment exerts a significant therapeutic effect after ischemia by augmenting collateral perfusion.
Journal of Cerebral Blood Flow & Metabolism (2012) **32,** 2012–2022; doi:10.1038/jcbfm.2012.102; published online 11 July 2012

Keywords: collateral circulation; focal cerebral ischemia; hemodynamics; neuroprotection; reperfusion

Introduction

In the pathophysiology of ischemic stroke, the brain's collateral circulation exerts a key influence on the extent and severity of the ischemic lesion and the efficacy of spontaneous or therapeutically induced reperfusion (Liebeskind, 2010*b*; Shuaib *et al*, 2011). This research area is of particular current clinical relevance as reperfusion strategies using thrombolytic agents and mechanical clot-removing devices constitute therapeutic mainstays in the clinical management of acute ischemic stroke (Ahmed *et al*, 2010).

Nonclot-removing neuroprotective strategies may also contribute to the restoration of blood flow to the ischemic brain by influencing its collateral circulation—an approach termed 'collateral therapeutics' (Liebeskind, 2010*b*). High-dose human albumin (ALB) therapy has emerged as a potent neuroprotective agent in experimental studies (Belayev *et al*, 1998, 2001) and preliminary clinical investigations of ischemic stroke (Palesch *et al*, 2006; Hill *et al*, 2011) and is now under study in an international phase III multicenter clinical efficacy trial—the ALIAS (Albumin in Acute Stroke) Trial (NIH ClinicalTrials.gov Identifier NCT00235495). Among its many potentially therapeutic actions, ALB appears to exert several important beneficial hemodynamic and intravascular effects. These include its endothelial binding and promotion of transcytosis (He and Curry, 1993); decreasing red-cell sedimentation under low-flow conditions (Peters, 1996); platelet antiaggregatory effects (Gresele *et al*, 1984); regulation of vascular tone via S-nitrosothiol formation (Keaney *et al*, 1993); diminishing neutrophil extravasation (Powers *et al*, 2003); and intravascular volume expansion and hemodilution (Belayev *et al*, 1998). In focal ischemia, we have shown that ALB improves

Correspondence: Professor MD Ginsberg, Department of Neurology (D4-5), University of Miami Miller School of Medicine, PO Box 016960, Miami, FL 33101, USA.
E-mail: mginsberg@med.miami.edu
[4]Current address: Department of Molecular and Integrative Physiology, University of Michigan, Ann Arbor, MI, USA.
Received 3 May 2012; revised 12 June 2012; accepted 13 June 2012; published online 11 July 2012

cerebral blood flow (CBF) to the ischemic core and penumbra (Huh *et al*, 1998); reverses postischemic intravascular stagnation and corpuscular adherence in the postcapillary microcirculation (Belayev *et al*, 2002); improves flow velocity distal to an occlusive arteriolar thrombus (Nimmagadda *et al*, 2008); and enhances the arteriolar flow velocity-augmenting effect of a thrombolytic agent (Park *et al*, 2008).

The objectives of the present study were (1) to characterize the spatial extent and intensity of cortical ischemia over time after occlusion of the distal middle cerebral artery (MCA); (2) to assess the therapeutic influence of ALB on these variables; and (3) to determine the manner in which the effect of ALB depends on the degree of preexisting collateralization. To this end, we used two inbred mouse strains that differ markedly in collateral circulation: the BALB/c strain, in which leptomeningeal collaterals are sparse (Zhang *et al*, 2010; Chalothorn and Faber, 2010; DeFazio *et al*, 2011), and the CD-1 strain, which possesses an intermediate degree of brain collateralization compared with the highly collateralized C57BL/6 and the sparsely collateralized BALB/c mouse strains (M Theus and RA DeFazio, unpublished data). Distal MCA branch occlusion was induced by quantum dot-facilitated laser occlusion (DeFazio *et al*, 2011). The temporal course of CBF in relation to ischemia and treatment was quantified by laser speckle contrast (LSC) imaging—a method that permitted sequential CBF monitoring and display with high spatial resolution (Boas and Dunn, 2010; Dunn, 2012) and has been successfully applied to study cerebrovascular physiology and pathophysiology in focal cerebral ischemia and other settings (Dunn *et al*, 2001; Dunn, 2012).

Materials and methods

Animal Preparation

These studies were conducted in male retired-breeder BALB/c and CD-1 mice aged 4 to 6 months (Charles River Laboratories, Wilmington, MA, USA). All procedures were approved by the University of Miami's Institutional Animal Care and Use Committee and were conducted in compliance with the Association for Assessment and Accreditation of Laboratory Animal Care guidelines. Anesthesia was induced with 2% isoflurane in an induction box (Braintree Scientific, Braintree, MA, USA) and was adjusted to the minimal isoflurane level needed to maintain full anesthesia as tested by the response to paw pinch (Ohio isoflurane vaporizer, Parkland Scientific, Coral Springs, FL, USA; vacuum recapture system, Harvard Apparatus, Holliston, MA, USA). Animals were placed on a warming pad regulated by a temperature controller (Fine Science Tools, Foster City, CA, USA) and were positioned within the anesthesia cone of the isoflurane vacuum recapture tube. A rectal probe was inserted for temperature control during surgery (heating pad and controller TR-200; Fine Science Tools, North Vancouver, BC, Canada). Catheters were inserted into a femoral artery and femoral vein (MicroRenathane tubing; Braintree Scientific) for blood-gas and blood-pressure monitoring and for intravenous delivery of ALB or saline, respectively. Further experimental details are provided in DeFazio *et al* (2011).

Animals were placed in a custom-built stereotaxic device (described in DeFazio *et al*, 2011) and the head was secured by ear bars. Anesthetic gases were delivered via a nose cone. The scalp and associated connective tissue were separated from the skull along the midline $\sim$1 to 2 mm anterior to bregma and 2 to 3 mm posterior to lambda. A needle temperature probe was inserted to monitor ipsilateral temporalis muscle temperature, which was regulated with a custom-built controller and an infrared heating lamp. A small amount of sterilized mineral oil was applied to the skull to prevent drying. A microdrill with a 1-mm carbide ball bit was used to thin the skull gently only over an area of approximately 1 to 2 mm^2 overlying the distal MCA branch of interest while the skull was cooled with mineral oil; the general approach of Yang *et al* (2010) was followed (detailed description in DeFazio *et al*, 2011). The outer skull layer and subjacent spongy bone were removed, permitting the pial arteries to be visualized through the remaining thin layer of bone.

Laser Occlusion System

The system described by DeFazio *et al* (2011) was used with minor modifications. In brief, the laser system consisted of a continuous wave diode-pumped Nd:YAG solid-state laser with 100 mW maximal output power at the frequency-doubled wavelength of 532 nm, with 2 mm output beam diameter (OEM Laser Systems, East Lansing, MI, USA). A laser power meter was used to determine the analog voltages required to deliver 40 mW at the target. Other components included a Uniblitz shutter and controller, a beam expander, cylindrical lenses, and a beam positioner; the details have been published (DeFazio *et al*, 2011). The system was mounted on a 750-mm optical rail oriented at a 13-degree angle from the vertical to ensure that the laser beam was perpendicular to the skull surface overlying the imaged area. (The experimental rig is depicted in the Supplementary Figure.)

To study infarction after distal MCA branch occlusion, we used the recently developed model of quantum dot-facilitated laser occlusion of a single pial artery (DeFazio *et al*, 2011). The largest MCA branch running from the lateral edge toward the medial axis between lambda and bregma was selected. After the skull over the MCA branch of interest was thinned, nonfunctionalized quantum dots (eFluor 650NC; eBiosciences, San Diego, CA, USA) were injected intravenously (0.1 to 0.25 μL/g body weight). A 40×100 μm laser line formed by crossed cylindrical lenses was focused within the MCA branch using the 532-nm laser at $\sim$1 mW under direct observation with a surgical stereo microscope. To occlude the vessel, laser power was increased to 40 mW and delivered in 500 to 750 ms pulses at 1 Hz (regulated by the shutter). Ten pulses were usually sufficient to occlude the vessel permanently. Complete occlusion was verified by the appearance of a white clot visible with a surgical microscope, and by LSC imaging.

The fluorescence properties of quantum dots allowed precise positioning of the laser beam, and their lack of membrane binding is thought to limit damage to platelets during photothrombotic vascular occlusion (DeFazio *et al*, 2011). In every animal, persistent occlusion was confirmed at 3 days by both visual inspection and laser-speckle imaging. No recanalization was detected in any of the animals of this study. In a parallel study (DeFazio, unpublished), repeated observations were made out to 7 days, indicating that the clot is indeed permanent in this time window.

Laser Speckle Contrast Imaging and Analysis

The laser speckle system was comprised of a Sanyo 785 nm diode laser and controller (Thorlabs, Newton, NJ, USA); and an infrared-sensitive camera (QICAM-IR, QImaging, Surrey, BC, Canada) fitted with a variable 0.5 to 6.5 × zoom lens assembly (Zoom 6000, Navitar, Rochester, NY, USA) and 785 nm laser-line band pass filter. Image Pro Plus (v5.1, Media Cybernetics, Bethesda, MD, USA) was used for image acquisition. All devices were mounted on rods attached to the main plate of the custom stereotaxic device. The system rested on a vibration-isolation table (TMC, Peabody, MA, USA). The skull was rotated to optimize the imaging plane. Although the depth of field in this wide-field imaging system was several millimeters, the effective depth of field was essentially superficial (i.e., we imaged a thick volume but visualized only the top of the scattering surface, as discussed in Ayata *et al*, 2004). The LSC imaging was conducted repeatedly throughout the experiment up to ~90 minutes or more after MCA branch occlusion. The image acquisition and analysis software package, ImageJ, was used for image processing (http://rsbweb.nih.gov/ij/). The macro routine 'Transform' (published in DeFazio *et al*, 2011) was used to convert raw images into LSC images. Using a 2 × 2-pixel filter, we obtained the inverse of the squared contrast ($p = \mu^2/\sigma^2$, where p is the new pixel value, μ is the local mean intensity, and σ is the local standard deviation of the intensity).

Speckle contrast K is a function of camera exposure-time T and is related to the autocovariance of the intensity fluctuations $C_i(\tau)$ (Dunn *et al*, 2001; Boas and Dunn, 2010) by the equation

$$K^2 = \sigma^2(T)/\mu^2 = 1/T\mu^2 \int_0^T C_i(\tau)d\tau$$

τ_c, the correlation time, which is assumed to be inversely and linearly proportional to flow of the scattering particles, was computed from equation 3 in Dunn *et al* (2001):

$$K = [(\tau_c/2T)\{1 - \exp(-2T/\tau_c)\}]^{0.5}$$

The resulting images depict the inverse of relative flow, with high-flow regions appearing bright, and low-flow regions dark. Stacks of 300 sequential raw images (each acquired with a 7-ms exposure separated by a 50-ms interval) were processed to produce each LSC image. It was possible, in this manner, to generate sequential LSC images (stacks) at intervals as short as 15 s throughout the entire experiment. Below, we use the term 'image' to refer to the average of 300 frames. The full frame of the LSC images measured 9.85 × 7.39 mm.

For analysis of flow trends over time, it was crucial that the sequential images be precisely coaligned to correct for small drifts in skull position over the course of the ~90-minute imaging period. The linear-affine transformation method (Zhao *et al*, 1993) or the piecewise affine-transformation method (Zhao *et al*, 2011) was used for this purpose. In each animal, three or more vessel-branching points were chosen as fiduciary points-of-reference. When more than three branching points were selected, image registration was conducted following the Delaunay triangulation structure, which matched each corresponding triangle formed by three branching points in sequential speckle images in a piecewise manner (Zhao *et al*, 2011). Image alignment was conducted on a PC with system parameters of 3 GHz CPU and 2 GB RAM.

The aligned images could then be arithmetically manipulated on a pixel-by-pixel basis. First, a baseline flow image was obtained by averaging, on a pixel-by-pixel basis, three images acquired ~1 to 4 minutes before initiation of MCA branch occlusion. Each subsequent image was then arithmetically manipulated, pixel-by-pixel, as follows to yield a difference image:

(Difference image pixel value) = ((current pixel value)–(baseline pixel value))/(baseline pixel value)

On visual inspection, satisfactory image alignment was attested to by the fact that difference images at baseline appeared completely black and featureless. Postocclusion difference images clearly revealed the spatial distribution and intensity of ischemia (Figure 1). The following pixel-based arithmetic manipulation was then performed on difference images (via ImageJ) to yield image data sets whose pixel values were numerically equal to fractional relative flow:

(Fractional relative flow of a pixel) = 1/((difference image pixel value) + 1)

These values, measured in regions-of-interest (ROIs) configured as described in Results, were used to analyze changes in relative flow over time.

Treatment

At 30 minutes after the induction of complete distal MCA branch occlusion, animals were treated with either 25% human ALB (Plasbumin-25, Talecris Biotherapeutics, Inc., Research Triangle Park, NC, USA) or with an equivalent volume of isotonic (0.9%) saline solution. BALB/c mice received 1.25 g/kg of ALB (or equivalent volume of saline) delivered intravenously over 5 minutes. CD-1 mice received 2.5 g/kg of ALB (or equivalent volume of saline) delivered over 10 minutes. The rationale for these differing doses was the following: both the 1.25 and the 2.50 g/kg doses of 25% ALB have been shown to be highly neuroprotective in experimental models of MCA occlusion (Belayev *et al*, 1998, 2001). In designing the current study, however, we suspected that the more highly collateralized (and therefore more infarct-resistant) CD-1 strain might be less susceptible

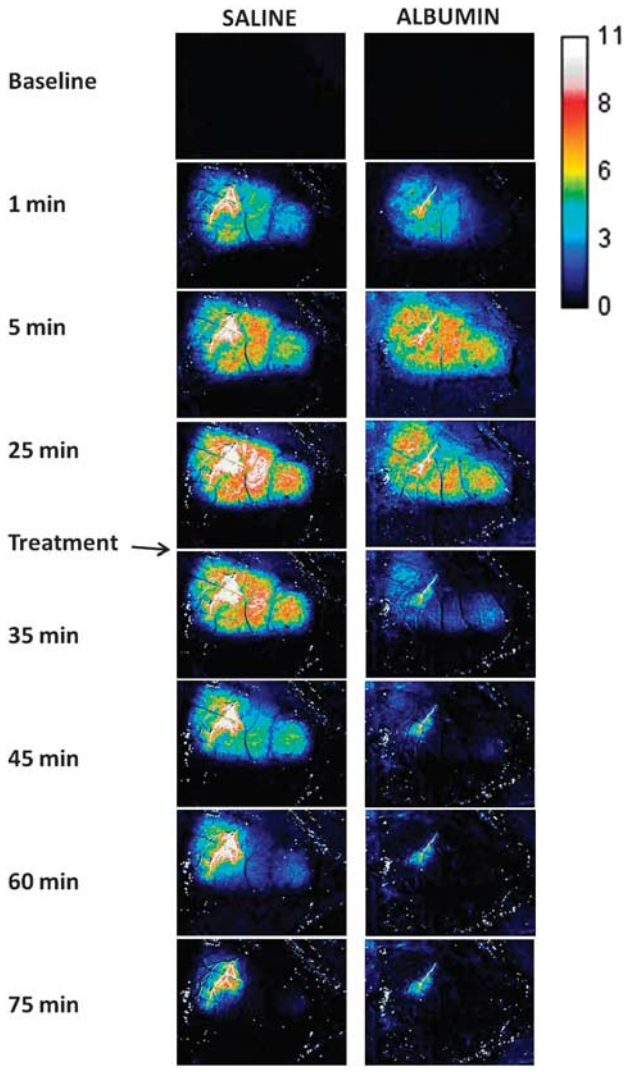

Figure 1 Difference images showing *the inverse of fractional relative flow* in BALB/c mice after distal middle cerebral artery (MCA) branch occlusion, and after treatment with either albumin (ALB) or saline.

to an effect of administered ALB, and therefore we wished to give it the benefit of the higher dose.

Morphological Studies

Animals were cardiac-perfused under deep isoflurane anesthesia on the third day after occlusion. Infarct size was assessed in BALB/c mice by triphenyl tetrazolium chloride (TTC) staining. CD-1 mice (and selected BALB/c mice) were perfusion fixed with 4% formaldehyde, and brains were stored in 4% formaldehyde for 24 to 48 hours and then in saline before postmortem magnetic resonance imaging (MRI).

Triphenyl Tetrazolium Chloride Staining

Triphenyl tetrazolium chloride (TTC, 1% solution) was prepared 30 minutes before use and warmed to 35°C. After saline cardiac perfusion, brains were removed into ice-cold saline for 5 minutes, and the entire brain was sectioned at 1 mm in a brain matrix, yielding six to eight sections which were placed in the TTC solution for 10 minutes at 35°C, then transferred to 4% formaldehyde at room temperature. Thirty-to-sixty minutes after fixation, a flat-bed scanner was used to acquire images of both faces of each section. Because of significant interanimal variation in the territory of the occluded distal MCA branch, it was not possible to control the precise location of the infarct, which appeared at somewhat different levels even within the same group.

Magnetic Resonance Imaging Methods

Ex-vivo MRI was performed on a Bruker Advance 11.7T system (Bruker Biospin, Billerica MA, USA) with a volumetric radiofrequency coil. Lesion volume from individual mouse brains was assessed using a T2-weighted 3D RARE acquisition with the following parameters: repetition time/echo time: 2,436.8 ms/7.9 ms; matrix: 256×256; field of view: 20 mm^3, with a single average. The 3D data set was reconstructed using 256 slices; each slice had a thickness of 7.8 μm. Total acquisition time was 1 hour.

Magnetic Resonance Imaging Analysis

Cheshire (Hayden Image/PAREXEL International Corp., Boulder, CO, USA) image-processing software was used semiautomatically to outline the whole brain on 3D RARE images. The whole brain was defined as extending from the first (anterior) slice in which the frontal association cortex was visible to the slice in which the posterior cortex was no longer visible. Ischemic lesions were identified as regions of either hyperintensity or hypointensity that differed from the surrounding normal-appearing cortical tissues. Brain and lesion volumes (mm^3) were extracted to Excel where lesion volumes (% of brain volume) were normalized to brain volumes to control for brain-size differences among animals. Finally, to visualize the rostro-caudal extent of the lesions, 3D volumetric reconstructions were performed using Amira (Mercury Computer Systems, Chelmsford, MA, USA).

Statistical Methods

Relative flow data over time in ALB- versus saline-treated mice were analyzed by two-way repeated-measures analysis of variance (ANOVA) with appropriate *post hoc* methods (Bonferroni, Holm-Sidak) to correct for multiple comparisons. Nonparametric comparisons were performed with the Mann–Whitney rank sum test. SigmaPlot software was used for display and statistical analysis (Systat Software Inc., San Jose, CA, USA). Exact P values are given when <0.05, and otherwise are denoted as 'not significant' (NS).

Results

Physiological variables for the two mouse strains are shown in Table 1. Blood pressure was measured

Table 1 Physiological variables

	Rectal T, °C	*Cranial T, °C*	*pH (units)*	*pCO_2, mm Hg*	*pO_2, mm Hg*
BALB/c, saline	37.6 ± 1.4	36.8 ± 0.3	7.362 ± 0.097	39.4 ± 7.4	181 ± 40
BALB/c, ALB	37.0 ± 1.1	36.7 ± 0.3	7.392 ± 0.031	40.1 ± 7.9	149 ± 44
CD-1, saline	38.2 ± 0.7	37.2 ± 0.2	7.384 ± 0.111	29.4 ± 12.9	187 ± 54
CD-1, ALB	37.9 ± 0.6	37.1 ± 0.2	7.568 ± 0.030[a]	18.2 ± 3.3	201 ± 15

ALB, albumin.
[a]$P < 0.05$ versus CD-1, saline, *t*-test.

in a subset of animals; the overall average was 71 ± 12 mm Hg. In the CD-1 series, moderate respiratory alkalosis was apparent in these spontaneously breathing mice.

Blood Flow—BALB/c Series

Figure 1 shows laser-speckle inverse-flow difference images in representative BALB/c mice of the saline and ALB groups. At baseline, before MCA branch occlusion, difference images showed the expected absence of detail. Within 1 to 2 minutes after visual verification of successful complete laser-induced MCA branch occlusion, laser-speckle images in all mice revealed a perfusion deficit that appeared earliest and most densely in relation to the occluded MCA branch. Within the next several minutes, the flow deficit expanded to involve a sizeable ovoid-shaped zone of the ipsilateral hemisphere (Figure 1). After administration of either saline or ALB at 30 minutes after occlusion, saline-treated mice showed a slight, gradual improvement in relative flow over the subsequent hour, while ALB-treated mice underwent a prompt and more pronounced improvement in relative flow.

Relative flow over time was measured in two contiguous ROIs: (1) *a centrally placed ROI*, consisting of a 150 × 150-pixel square (~2.1 × 2.1 mm) positioned in an unbiased manner so as to include the entire proximal portion of the occluded MCA branch with its origin at the superior edge of the square; and (2) *a peripherally placed ROI*, consisting of a 250 × 150-pixel rectangle (~2.1 × 3.5 mm) positioned contiguous to the central ROI. The placement of ROIs is shown in Figure 2.

The time course of relative flow measured in the two ROIs is plotted in Figure 3. *In the centrally placed (square)* ROI (Figure 3A), flow declined sharply in all animals over the first 1 to 4 minutes after vascular occlusion, attaining stable flow levels of 13 ± 4% and 14 ± 4% of baseline (mean ± s.d.) in the saline and ALB groups, respectively, at 5 to 25 minutes after occlusion; these values did not differ statistically between groups. After ALB or saline treatment at 30 minutes after occlusion, flow in the central ROI rose slowly and modestly in the saline-treated group, but more extensively in ALB-treated animals, so that mean flow in the ALB group

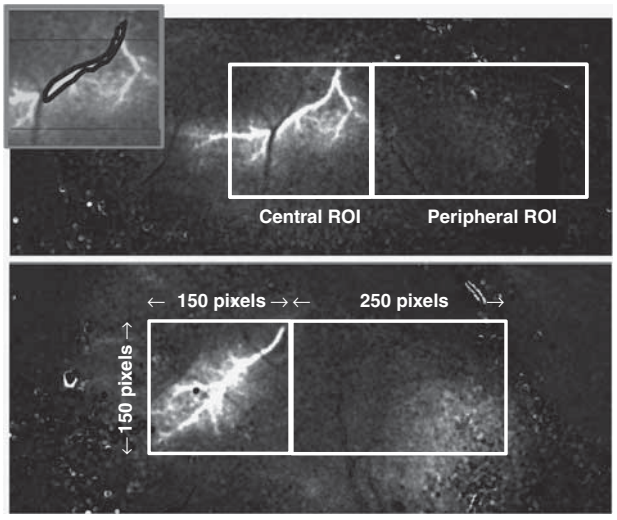

Figure 2 Difference images immediately after distal middle cerebral artery (MCA) occlusion in representative BALB/c mice of the saline (upper panel) and albumin (ALB) (lower panel) series, showing the positioning of the 150 × 150-pixel square central region-of-interest (ROI) and the contiguous, 250 × 150-pixel rectangular peripheral ROI. (Rostral pole is to the right.) Inset shows an irregular polygon-ROI positioned so as to estimate relative flow in the proximal portion of the occluded artery itself.

exceeded that in the saline group at all posttreatment time points (Figure 3A). Two-way repeated-measures ANOVA confirmed a significant effect of treatment ($F_{1,9} = 6.11$, $P = 0.035$) and a highly significant treatment × time interaction ($P < 0.001$). Bonferroni comparisons revealed significant differences by treatment group at time points 45 through 90 minutes, with highly significant differences at 70 minutes and beyond ($P \leqslant 0.002$). In the interval 60 to 90 minutes (i.e., at 30 to 60 minutes after treatment), median relative flow in the central ROI of the saline group was 28.9% of baseline, compared with 57.9% of baseline in the ALB group, amounting to a 2-fold ALB-induced flow increase relative to saline (P = NS, Mann–Whitney rank sum test) (Figure 4).

As the proximal portion of the occluded MCA branch constituted a portion of the central ROI, we analyzed relative flow within this vascular segment itself by means of an ROI drawn to conform to the proximal portion of the occluded artery but excluding the adjacent parenchyma. An illustrative ROI is

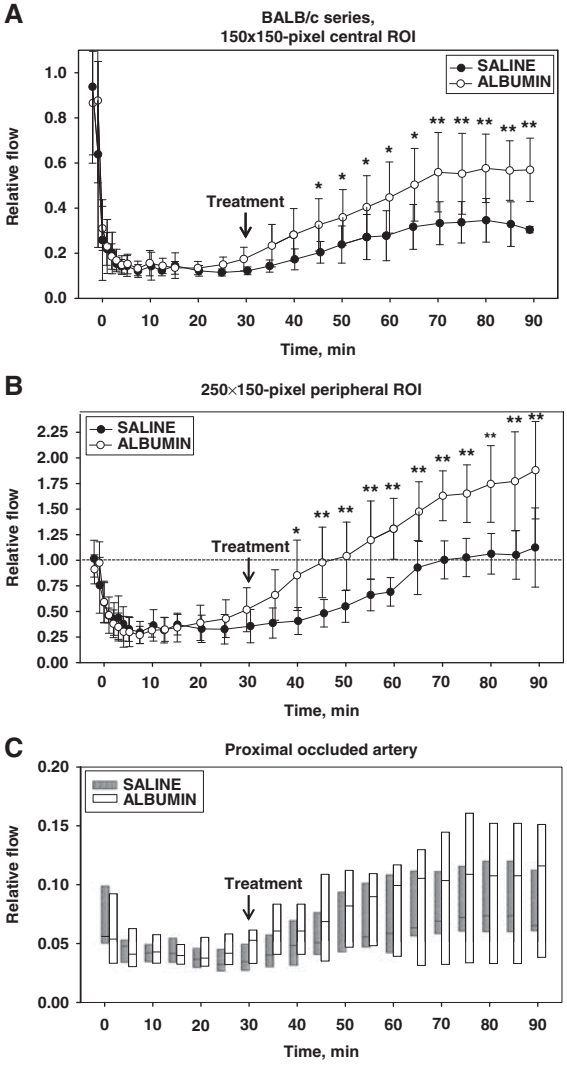

Figure 3 *Fractional flow relative to preischemic baseline* in central (**A**) and peripheral (**B**) regions-of-interest (ROIs), and in the proximal segment of the occluded artery (**C**) of BALB/c mice after middle cerebral artery (MCA) branch occlusion and treatment (at 30 minutes) with either albumin (ALB) or saline. The boxes in (**C**) show median values and the 5th to 95th percentile ranges. $^{*}P < 0.05$; $^{**}P \leqslant 0.001$, two-way repeated-measures analysis of variance (ANOVA) followed by Bonferroni tests.

shown in Figure 2 (inset), and the flow measurements are shown in Figure 3C. Repeated-measures ANOVA failed to reveal a significant effect of ALB treatment on flow in the proximal occluded vessel itself (P = NS), and an absence of treatment × time interaction (P = NS). Nonetheless, *median* arterial flow at posttreatment times (35 to 90 minutes) tended to be consistently higher in ALB-treated mice than in saline-treated animals ($P = 0.004$, Mann–Whitney rank sum test). Median relative flow values at 35 to 90 minutes averaged 0.093 versus 0.063 in ALB- versus saline-treated mice, or a 47% ALB-related relative improvement. Taken together with the central ROI measurements, these results indicate

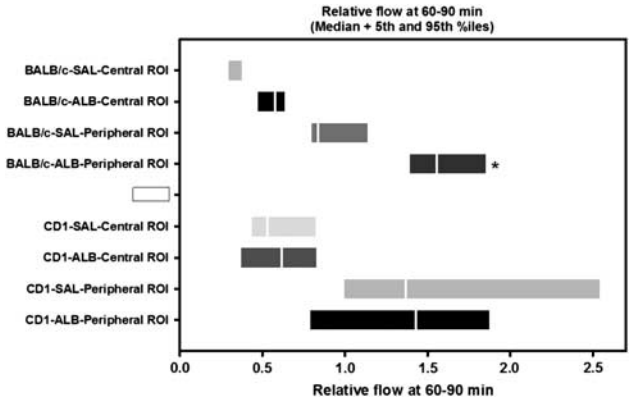

Figure 4 Relative flow at 60 to 90 minutes after middle cerebral artery (MCA) branch occlusion in BALB/c and CD-1 mice treated (at 30 minutes) with either ALB or saline (SAL). Median values and 5th to 95th percentile ranges are shown for the central and peripheral regions-of-interest (ROIs). $^{*}P < 0.05$ versus BALB/c-SAL-Peripheral ROI.

that a substantial ALB-induced increment in *parenchymal* flow occurred despite only a subtle treatment-induced flow increment in the occluded MCA branch itself; that is, ALB appeared to enhance parenchymal perfusion in the central ROI disproportionately to the slight perfusion increment in the feeding vessel itself.

In the peripherally positioned (rectangular) ROI—a zone thought to contain penumbra plus oligemic tissue—relative flow also declined promptly after arterial occlusion but to a lesser extent than in the centrally placed ROI (Figure 3B). At 5 to 25 minutes after occlusion, flow in the peripheral ROI declined in an identical manner to only 33 ± 13% and to 34 ± 13% of baseline in the saline and ALB groups, respectively. Over the hour after ALB or saline treatment at 30 minutes after occlusion, relative flow in the peripheral ROI increased gradually toward baseline levels in the saline group but rose much more extensively in the ALB group, attaining hyperemic levels at 60 minutes and beyond (Figure 3B). Thus, in the interval 60 to 90 minutes (i.e., 30 to 60 minutes after treatment), median relative flow had recovered to 83.7% of baseline in the saline group, but had risen to 156% of baseline in the ALB-treated group, amounting to a 1.9-fold ALB-induced relative increase ($P = 0.004$, Mann–Whitney rank sum test) (Figure 4). Two-way repeated-measures ANOVA revealed a significant effect of treatment ($F_{1,9} = 8.36$, $P = 0.018$) and a highly significant treatment × time interaction ($P < 0.001$). Bonferroni comparisons revealed significant treatment effects beginning at 40 minutes ($P = 0.003$) and continuing at all subsequent time points ($P \leqslant 0.001$) (Figure 3B).

Blood Flow—CD-1 Series

BALB/c mice express few leptomeningeal anastomoses, while CD-1 mice have an intermediate degree

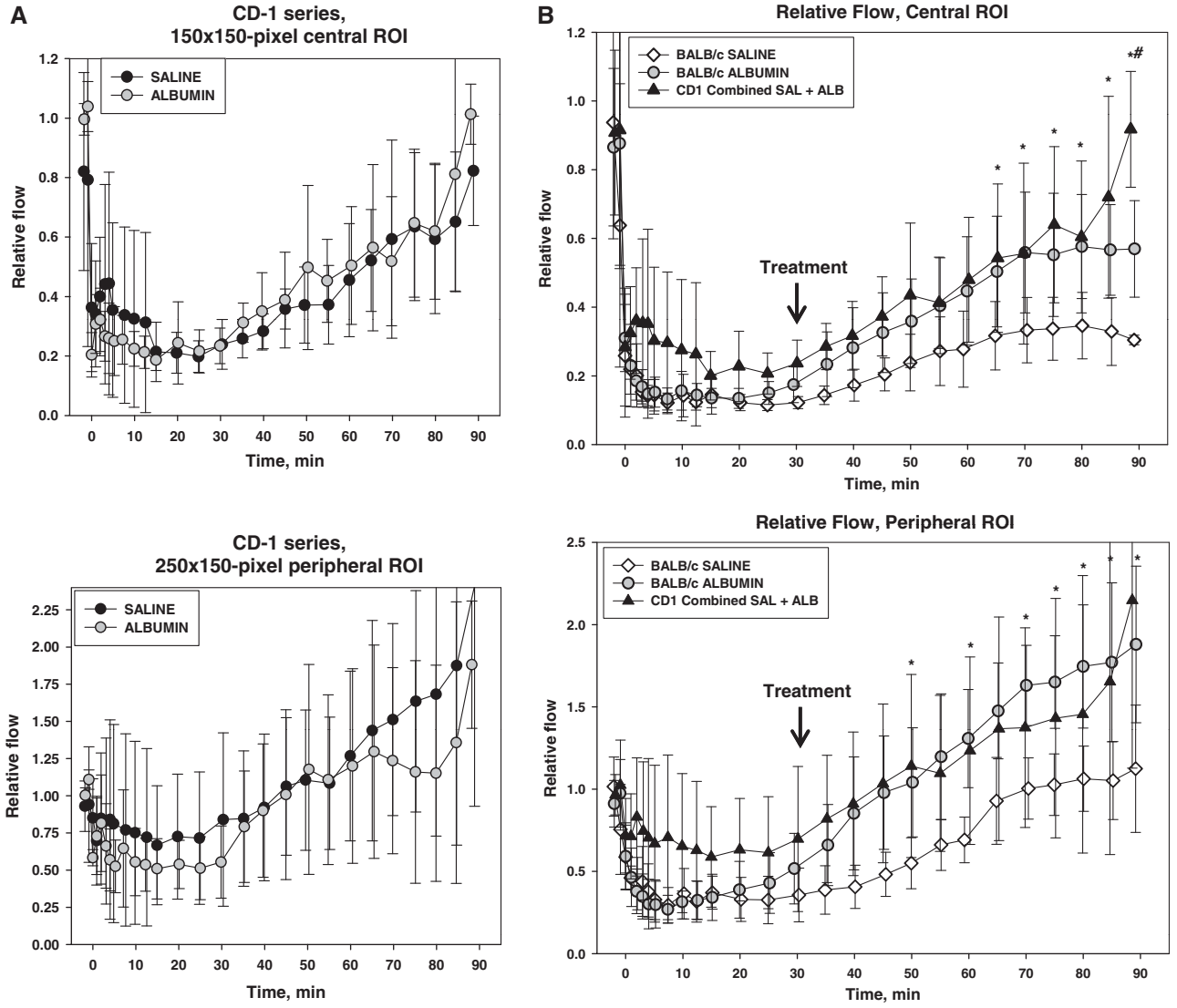

Figure 5 (**A**) Relative flow in central and peripheral regions-of-interest (ROIs), CD-1 series. (**B**) Relative flow (mean ± s.d.) shown separately for saline- and albumin-treated BALB/c mice, and for combined saline- plus albumin-treated animals of the CD-1 series. $^{*}P < 0.05$, CD-1 versus BALB/c SAL. $^{\#}P < 0.05$, CD-1 versus BALB/c ALB, Holm-Sidak tests.

of collateralization. Thus, we next asked whether collateral density modified the impact of ALB on postocclusion CBF dynamics. As in the BALB/c series, relative flow over time was measured in CD-1 mice in central and peripheral ROIs placed as shown in Figure 2. These results are plotted in Figure 5A. In contrast to the BALB/c series, relative flow in CD-1 mice behaved similarly over time after saline and ALB treatment. Repeated-measures ANOVA showed a significant effect of time ($P < 0.001$) but the absence of a treatment effect ($P = $ NS) and of a treatment × time interaction ($P = $ NS).

Flow was also measured in the proximal segment of the occluded MCA branch in the CD-1 mice. Repeated-measures ANOVA revealed no effect of ALB treatment on arterial flow ($P = $ NS), and an absence of treatment × time interaction ($P = $ NS). Mean arterial flow at posttreatment times (35 to 90 minutes) was similar in ALB- and saline-treated mice relative to preischemic baseline (mean ± s.d., 0.137 ± 0.067 and 0.127 ± 0.068, respectively; $P = $ NS, *t*-test).

Comparison of Flow in BALB/c and CD-1 Mice

Because relative flow in CD-1 mice after MCA branch occlusion and after treatment behaved similarly in ALB- and saline-treated animals, these two treatment groups were combined in Figure 5B, which compares relative flow in CD-1 mice with ALB- and saline-treated BALB/c mice. After MCA branch occlusion, CD-1 mice tended to develop less severe parenchymal ischemia than BALB/c animals. After treatment at 30 minutes, relative flow tended to be highest in CD-1 mice, intermediate

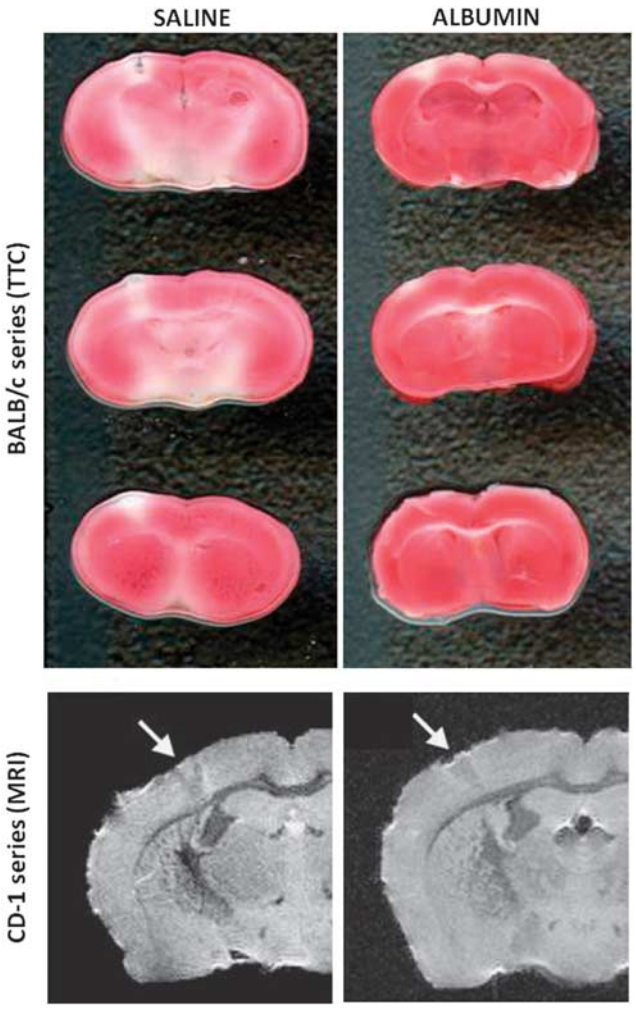

Figure 6 Upper panel: Triphenyl tetrazolium chloride (TTC)-stained sections showing the infarct in representative saline- and albumin (ALB)-treated BALB/c mice. Lower panel: T2-weighted magnetic resonance imaging (MRI) images in representative saline- and ALB-treated CD-1 mice.

in ALB-treated BALB/c mice, and lowest in saline-treated BALB/c mice in both the central and peripheral ROIs (Figure 5B). Flow values in the ROIs of CD-1 mice were significantly greater than in saline-treated BALB/c animals at various times from 50 to 90 minutes ($P < 0.05$, Holm-Sidak comparisons) (Figure 5B).

Morphological Observations, BALB/c Series

In nine mice of the BALB/c series (saline, $n = 4$; ALB, $n = 5$), TTC staining of the 1-mm coronally sectioned brain was successfully performed at 3 days after arterial occlusion. Representative TTC images are shown in Figure 6. Cortical infarct volumes estimated by planimetry of scanned images were 2.26 ± 0.42 and $1.23 \pm 0.66\,mm^3$ in saline- and ALB-treated mice, respectively (mean ± s.d.; $P = 0.03$ by *t*-test). On average, ALB treatment reduced cortical infarct volume by 45%.

Morphological Observations, CD-1 Series

Because infarct size in CD-1 mice was considerably smaller than in the BALB/c strain, we suspected that it would be nearly impossible to obtain reliable quantification via TTC. Thus, we turned to *ex-vivo* MRI imaging in the CD-1 series. Cortical infarct volume was quantified on T2-weighted MRI scans of seven brains (saline, $n = 4$; ALB, $n = 3$) perfusion fixed in 4% formaldehyde at 3 days after arterial occlusion. Mean infarct volume did not differ significantly by treatment (saline, $0.71 \pm 0.72\,mm^3$; ALB, $0.52 \pm 0.71\,mm^3$). For the entire CD-1 series, infarct volume averaged $0.63 \pm 0.66\,mm^3$. Figure 6, lower panel, shows representative MRI scans.

Discussion

The key observations of the present study are that, in BALB/c mice—a strain with sparse brain collaterals (Majid *et al*, 2000; Keum and Marchuk, 2009; Zhang *et al*, 2010; Chalothorn and Faber, 2010; DeFazio *et al*, 2011) – MCA branch occlusion led to severe CBF declines into the ischemic-core range (~13% to 14% of control) (Zhao *et al*, 1997; Belayev *et al*, 1997), and that subsequent ALB treatment produced significant downstream flow improvements in excess of those observed in saline-treated mice (Figure 3). This was the case both in the central ROI (encompassing the presumed ischemic core), where ALB treatment led to twofold median CBF increases from the penumbral to the benign-oligemic range; and in the peripheral ROI (the zone of presumed penumbra and benign oligemia), where postALB flow rose into the hyperemic range. (Unfortunately, whether any of the flow restitution observed was due in part to the nonspecific administration of fluids cannot be ascertained as we did not study untreated controls.) In contrast to BALB/c mice, in animals of the CD-1 strain, in which an intermediate degree of brain collateralization was present before ischemia, MCA branch occlusion led to less severe initial ischemia and ALB treatment failed to induce beneficial hemodynamic effects compared with saline-treated controls (Figure 5A).

It is improbable that the substantial ALB-induced improvements in parenchymal perfusion observed in BALB/c mice were attributable to the slight median perfusion increase noted in the proximal portion of the occluded MCA branch itself (Figure 3C). Rather, the data suggest that ALB treatment led, in BALB/c mice, to *a frank augmentation of collateral circulation*. This conclusion is supported by the fact that ALB treatment failed to increase perfusion in the CD-1 strain, in which adequate native collateral channels were already present (Figure 5A). Consistent with ALB's flow-enhancing effect in BALB/c but not in CD-1 mice, morphological analysis revealed diminished cortical infarct volume in ALB-treated BALB/c mice but not in the CD-1 strain (Figure 6).

The use of inbred mouse strains that differ substantially in their degree of brain collateralization was central to our experimental design. In a study of 15 inbred mouse strains, wide interstrain differences were found with respect to the numbers of collateral channels (range, 56-fold), as well as their diameters (range, threefold) and lengths (Zhang *et al*, 2010). Collateral numbers and diameters are ample in the C57BL/6 strain but much lower in BALB/c mice (Zhang *et al*, 2010; DeFazio *et al*, 2011), and there are marked differences in the extent of collateral development in these two strains during late embryonic and early postnatal ages (Chalothorn and Faber, 2010). Corresponding to these differences in the extent of collateralization, others have noted up to 30-fold variation in infarct volume among strains after permanent MCA occlusion (Majid *et al*, 2000; Keum and Marchuk, 2009), with highly significant inverse correlations between infarct volume and collateral numbers and diameters as well as numbers of penetrating arterioles (Zhang *et al*, 2010). DeFazio *et al* showed by vessel painting that anastomotic interconnections between major vascular territories were robust in C57BL/6J mice but only $\sim$20% to 30% as numerous in BALB/c mice; correspondingly, after distal MCA branch occlusion, mean infarction volume was $\sim$2.2 mm^3 in BALB/c mice, but $<$0.2 mm^3 in the C57BL/6J strain (DeFazio *et al*, 2011). Hereditable factors appear to account for around three quarters of the collateral differences among strains (Zhang *et al*, 2010). Detailed genetic analysis has identified three quantitative trait loci that modulate these differences, with a major locus on a small region of mouse chromosome 7, *Civq1,* accounting for over half of this variation; 12 candidate genes were identified (Keum and Marchuk, 2009). In the present study, we avoided the use of the C57BL/6 strain because of its abundant collateralization and tiny infarction volume, and, rather, chose to compare the BALB/c strain with the CD-1 strain, which in our preliminary vessel-painting studies showed an intermediate degree of native brain collateralization (Theus and DeFazio, unpublished).

It is evident from both animal and human investigations that the extent of collateral blood flow between the territories of feeding arteries is a major determinant of the extent and severity of stroke-related brain injury (Liebeskind, 2009*a*; Shuaib *et al*, 2011; DeFazio *et al*, 2011). Because collateral channels are often anatomically complex and involve small distal vessels, the traditional 'gold-standard' for their visualization in humans has been conventional catheter-based cerebral angiography (Liebeskind, 2009*a*)—an invasive method seldom used (or justified) before the onset of vascular symptoms or signs. Hence, our anatomic knowledge of the human brain's normal collateralization is woefully incomplete. More recently, less invasive imaging approaches such as CT angiography and magnetic resonance angiography have revealed that collateral anastomoses may be recruited quickly at the onset of ischemia, triggered by local elevations in fluid shear stress, and that they evolve in a dynamic manner in the first few hours (Liebeskind, 2009*a*). Events hypothesized to participate in this process include local venous collapse triggered by marginal arterial inflow, leading to increased downstream resistance, which in turn limits further arterial inflow by reducing cerebral perfusion pressure; this contributes to infarct growth, which may extend to the limit of a vascular territory or stop when CBF is sufficient to meet metabolic demands (Zhao *et al*, 1997; Belayev *et al*, 1997; Liebeskind, 2009*a*).

In clinical studies, stroke patients with less conspicuous collateral channels by CT angiography became symptomatic and came to hospital earlier than those with more robust collaterals (Maas *et al*, 2009). Diminished collaterals are predictive of clinical deterioration in patients with vascular occlusion (Liebeskind, 2009*b*), and collateral flow beyond a stenosis is a potent predictor of subsequent ischemia (Liebeskind, 2009*a*). In the large multicenter Warfarin-Aspirin Symptomatic Intracranial Disease trial, in subjects with stenoses of 70% to 99% the presence of more extensive collaterals lowered the risk of subsequent territorial stroke by $\sim$4- to 6-fold (Liebeskind *et al*, 2011).

While collateral perfusion beyond an occlusion aids recanalization (Liebeskind, 2009*a*), it is nonetheless the case that revascularization strategies designed to open an occluded artery (i.e., *recanalization*) may not necessarily result in effective parenchymal *reperfusion* (Liebeskind, 2010*a*) owing to the presence of resistance to downstream flow mediated by microcirculatory obstruction, endothelial injury (Barber *et al*, 2004), or dynamic changes in the venous circulation (Pranevicius *et al*, 2012). Although recanalization of occluded vessels in stroke patients leads to higher CT-perfusion indices of reperfusion (e.g., cerebral blood volume and mean transit time), even in patients without recanalization those with good collateral flow have higher reperfusion indices than those with poor collateral flow (Soares *et al*, 2010).

In human ischemic stroke, the time from *symptom* onset does not reflect the true time from stroke onset since symptoms only become manifest once collaterals fail to compensate for hypoperfusion, and the latter process is highly variable in individual patients (Liebeskind, 2009*a*). For this reason, effective thrombolytic strategies may be limited more by hemodynamic factors than by the characteristics of the clot itself. It is in this context that we believe the present results have their greatest therapeutic relevance. Previous studies from our laboratory point to major potentially beneficial hemodynamic effects of ALB therapy in focal ischemia: After temporary MCA occlusion in rats, confocal microscopy reveals the deposition of adherent material (presumed to consist of red cells, platelets, neutrophils, and fibrin) within cortical venules in the early reperfusion period; ALB reverses this phenomenon (Belayev *et al*, 2002). In

related studies, laser-induced occlusion of a single cortical arteriole results in a precipitous decline in downstream flow velocity within the occluded vessel (measured by 2-photon microscopy); subsequent saline administration fails to influence flow velocity, whereas ALB results in progressive increases in downstream flow velocity, suggesting the possible ALB-induced development of microchannels within or around the occlusive thrombus (Nimmagadda *et al*, 2008). In this same model, sublytic doses of the thrombolytic agent, reteplase, increase flow velocity modestly, while ALB therapy leads to a further additive flow-velocity augmentation (Park *et al*, 2008). In this context, it is worth noting that, even in patients thought to have 'complete' arterial occlusion, small channels of residual flow may persist along the clot's periphery, as evidenced by angiographic 'tram-tracking' (Otsuka *et al*, 2008; Liebeskind, 2009*a*).

In our pilot clinical trial of ALB therapy in acute ischemic stroke, patients receiving thrombolytic therapy with intravenous tPA showed a much greater neurologic improvement when treated with higher dose ALB than when receiving lower (presumed subtherapeutic) ALB doses (Ginsberg *et al*, 2006; Palesch *et al*, 2006). Reinforcing these observations, our subsequent exploratory efficacy analysis of data from thrombolysed subjects of the ALIAS Multicenter Part I Trial revealed that subjects receiving ALB showed a strong trend for improved clinical outcome compared with saline-treated subjects (Hill *et al*, 2011).

Taken together, our findings indicate that ALB therapy exerts consistent salutary influences on cerebrovascular hemodynamics within an ischemic zone. The key finding of the present study, that ALB treatment augments collateral perfusion to the ischemic field in a mouse strain severely deficient in patent collaterals (BALB/c), raises an important and intriguing question that will require further study: namely, to what extent might *latent* (i.e., anatomically present but nonfunctional) microvascular collaterals exist in the normal brain, which can be induced to become patent after ischemia via a therapeutic intervention such as ALB?

Disclosure/conflict of interest

The authors declare no conflict of interest.

References

Ahmed N, Wahlgren N, Grond M, Hennerici M, Lees KR, Mikulik R, Parsons M, Roine RO, Toni D, Ringleb P (2010) Implementation and outcome of thrombolysis with alteplase 3–4.5 hours after an acute stroke: an updated analysis from SITS-ISTR. *Lancet Neurol* 9:866–74

Ayata C, Dunn AK, Gursoy-Ozdemir Y, Huang Z, Boas DA, Moskowitz MA (2004) Laser speckle flowmetry for the study of cerebrovascular physiology in normal and ischemic mouse cortex. *J Cereb Blood Flow Metab* 24: 744–55

Barber PA, Foniok T, Kirk D, Buchan AM, Laurent S, Boutry S, Muller RN, Hoyte L, Tomanek B, Tuor UI (2004) MR molecular imaging of early endothelial activation in focal ischemia. *Ann Neurol* 56: 116–20

Belayev L, Liu Y, Zhao W, Busto R, Ginsberg MD (2001) Human albumin therapy of acute ischemic stroke: marked neuroprotective efficacy at moderate doses and with a broad therapeutic window. *Stroke* 32:553–60

Belayev L, Pinard E, Nallet H, Seylaz J, Liu Y, Riyamongkol P, Zhao W, Busto R, Ginsberg MD (2002) Albumin therapy of transient focal cerebral ischemia: *in vivo* analysis of dynamic microvascular responses. *Stroke* 33: 1077–84

Belayev L, Zhao W, Busto R, Ginsberg MD (1997) Transient middle cerebral artery occlusion by intraluminal suture: I. Three-dimensional autoradiographic image-analysis of local cerebral glucose metabolism-blood flow interrelationships during ischemia and early recirculation. *J Cereb Blood Flow Metab* 17:1266–80

Belayev L, Zhao W, Pattany PM, Weaver RG, Huh PW, Lin B, Busto R, Ginsberg MD (1998) Diffusion-weighted magnetic resonance imaging confirms marked neuroprotective efficacy of albumin therapy in focal cerebral ischemia. *Stroke* 29:2587–99

Boas DA, Dunn AK (2010) Laser speckle contrast imaging in biomedical optics. *J Biomed Opt* 15:011109

Chalothorn D, Faber JE (2010) Formation and maturation of the native cerebral collateral circulation. *J Mol Cell Cardiol* 49:251–9

DeFazio RA, Levy S, Morales CL, Levy RV, Dave KR, Lin HW, Abaffy T, Watson BD, Perez-Pinzon MA, Ohanna V (2011) A protocol for characterizing the impact of collateral flow after distal middle cerebral artery occlusion. *Transl Stroke Res* 2:112–27

Dunn AK (2012) Laser speckle contrast imaging of cerebral blood flow. *Ann Biomed Eng* 40:367–77

Dunn AK, Bolay H, Moskowitz MA, Boas DA (2001) Dynamic imaging of cerebral blood flow using laser speckle. *J Cereb Blood Flow Metab* 21:195–201

Ginsberg MD, Hill MD, Palesch YY, Ryckborst KJ, Tamariz D (2006) The ALIAS Pilot Trial: a dose-escalation and safety study of albumin therapy for acute ischemic stroke. I. Physiological responses and safety results. *Stroke* 37:2100–6

Gresele P, Deckmyn H, Huybrechts E, Vermylen J (1984) Serum albumin enhances the impairment of platelet aggregation with thromboxane synthase inhibition by increasing the formation of prostaglandin D2. *Biochem Pharmacol* 33:2083–8

He P, Curry FE (1993) Albumin modulation of capillary permeability: role of endothelial cell $[Ca^{2+}]_i$. *Am J Physiol* 265:H74–82

Hill MD, Martin RH, Palesch YY, Tamariz D, Waldman BD, Ryckborst KJ, Moy CS, Barsan WG, Ginsberg MD (2011) The Albumin in Acute Stroke Part 1 Trial: an exploratory efficacy analysis. *Stroke* 42:1621–5

Huh PW, Belayev L, Zhao W, Busto R, Saul I, Ginsberg MD (1998) The effect of high-dose albumin therapy on local cerebral perfusion after transient focal cerebral ischemia in rats. *Brain Res* 804:105–13

Keaney JFJ, Simon DI, Stamler JS, Jaraki O, Scharfstein J, Vita JA, Loscalzo J (1993) NO forms an adduct with serum albumin that has endothelium-derived relaxing factor-like properties. *J Clin Invest* 91:1582–9

Keum S, Marchuk DA (2009) A locus mapping to mouse chromosome 7 determines infarct volume in a mouse model of ischemic stroke. *Circ Cardiovasc Genet* 2:591–8

Liebeskind DS (2009a) Imaging the future of stroke: I. Ischemia. *Ann Neurol* 66:574–90

Liebeskind DS (2009b) Stroke: the currency of collateral circulation in acute ischemic stroke. *Nat Rev Neurol* 5:645–6

Liebeskind DS (2010a) Recanalization and reperfusion in acute ischemic stroke. *F1000 Med Rep* 2:pii: 71

Liebeskind DS (2010b) Reperfusion for acute ischemic stroke: arterial revascularization and collateral therapeutics. *Curr Opin Neurol* 23:36–45

Liebeskind DS, Cotsonis GA, Saver JL, Lynn MJ, Cloft HJ, Chimowitz MI (2011) Collateral circulation in symptomatic intracranial atherosclerosis. *J Cereb Blood Flow Metab* 31:1293–301

Maas MB, Lev MH, Ay H, Singhal AB, Greer DM, Smith WS, Harris GJ, Halpern E, Kemmling A, Koroshetz WJ, Furie KL (2009) Collateral vessels on CT angiography predict outcome in acute ischemic stroke. *Stroke* 40:3001–5

Majid A, He YY, Gidday JM, Kaplan SS, Gonzales ER, Park TS, Fenstermacher JD, Wei L, Choi DW, Hsu CY (2000) Differences in vulnerability to permanent focal cerebral ischemia among 3 common mouse strains. *Stroke* 31: 2707–14

Nimmagadda A, Park H-P, Prado R, Ginsberg MD (2008) Albumin therapy improves local vascular dynamics in a rat model of primary microvascular thrombosis: a two-photon laser-scanning microscopy study. *Stroke* 39: 198–204

Otsuka Y, Waki R, Yamauchi H, Fukazawa S, Kimura K, Shimizu K, Fukuyama H (2008) Angiographic demarcation of an occlusive lesion may predict recanalization after intra-arterial thrombolysis in patients with acute middle cerebral artery occlusion. *J Neuroimaging* 18: 422–7

Palesch YY, Hill MD, Ryckborst KJ, Tamariz D, Ginsberg MD (2006) The ALIAS Pilot Trial: a dose-escalation and safety study of albumin therapy for acute ischemic stroke. II. Neurological outcome and efficacy-analysis. *Stroke* 37:2107–14

Park HP, Nimmagadda A, DeFazio RA, Busto R, Prado R, Ginsberg MD (2008) Albumin therapy augments the effect of thrombolysis on local vascular dynamics in a rat model of arteriolar thrombosis: a two-photon laser-scanning microscopy study. *Stroke* 39:1556–62

Peters Jr T (1996) *All About Albumin. Biochemistry, Genetics, and Medical Applications*. San Diego: Academic Press

Powers KA, Kapus A, Khadaroo RG, He R, Marshall JC, Lindsay TF, Rotstein OD (2003) Twenty-five percent albumin prevents lung injury following shock/resuscitation. *Crit Care Med* 31:2355–63

Pranevicius O, Pranevicius M, Pranevicius H, Liebeskind DS (2012) Transition to collateral flow after arterial occlusion predisposes to cerebral venous steal. *Stroke* 43:575–9

Shuaib A, Butcher K, Mohammad AA, Saqqur M, Liebeskind DS (2011) Collateral blood vessels in acute ischaemic stroke: a potential therapeutic target. *Lancet Neurol* 10: 909–21

Soares BP, Tong E, Hom J, Cheng SC, Bredno J, Boussel L, Smith WS, Wintermark M (2010) Reperfusion is a more accurate predictor of follow-up infarct volume than recanalization: a proof of concept using CT in acute ischemic stroke patients. *Stroke* 41:e34–40

Yang G, Pan F, Parkhurst CN, Grutzendler J, Gan WB (2010) Thinned-skull cranial window technique for long-term imaging of the cortex in live mice. *Nat Protoc* 5:201–8

Zhang H, Prabhakar P, Sealock R, Faber JE (2010) Wide genetic variation in the native pial collateral circulation is a major determinant of variation in severity of stroke. *J Cereb Blood Flow Metab* 30:923–34

Zhao W, Belayev L, Ginsberg MD (1997) Transient middle cerebral artery occlusion by intraluminal suture: II. Neurological deficits, and pixel-based correlation of histopathology with local blood flow and glucose utilization. *J Cereb Blood Flow Metab* 17:1281–90

Zhao W, Shen Q, Belayev L, Ginsberg MD (2011) Edema effect correction by image analysis to estimate infarction volume for animal MCAo models. *Proceedings of 25th International Symposium on Cerebral Blood Flow, Metabolism and Function*. Barcelona, Spain, 2011, p314

Zhao W, Young TY, Ginsberg MD (1993) Registration and three-dimensional reconstruction of autoradiographic images by the disparity analysis method. *IEEE Trans Med Imaging* 12:782–91

Supplementary Information accompanies the paper on the Journal of Cerebral Blood Flow & Metabolism website (http://www.nature.com/jcbfm)